

RESEARCH

Open Access



Unravelling protein corona formation on pristine and leached microplastics

Amanda Louise Dawson^{1,2*}, Utpal Bose^{1,2}, Dongdong Ni¹ and Joost Laurus Dinant Nelis¹

Abstract

Upon entering the environment, the surface properties of pristine plastics are rapidly altered due to interactions with exogenous biomolecules, contaminants, and even microbiota, which ultimately alter their ecological impacts. When present in biological fluids or high protein environments, micro(nano)plastics bind with proteins, which form a protein corona around the particle. Although a significant body of literature exists on protein corona formation on nanomaterials, less is known about how the physiochemical properties of microplastics may influence protein corona formation. This study utilises quantitative proteomics to quantify protein binding to pristine and leached microplastics. Pristine polyethylene (PE) beads (50 and 500 μm), polyamide (PA) fibres (100 μm), polyethylene terephthalate fibres (500 μm), and fragments (< 300 μm), as well as pristine and leached textile microfibrils comprised of PET, recycled PET, PA or cotton were incubated for 24 h in bovine serum albumin solution (2 mg mL⁻¹) to form a protein corona. Protein adsorption to microplastics was dependant on particle surface area to volume ratio but only when additives were absent. For environmentally relevant textile microfibrils, cotton microfibrils adsorbed significantly more protein than synthetic microfibrils. Fourteen-day aqueous leaching increased the zeta potential of all microfibrils. However, only PA fibres adsorbed significantly higher protein on the leached fibres compared to their pristine counterparts. Overall, the presence of chemical additives in microplastics strongly influenced protein corona formation, and this phenomenon should be incorporated into routine microplastic toxicity assessment.

Keywords Microplastics, Nanoplastics, Leachates, Ecocorona, Environmentally relevant, Microfibre

*Correspondence:

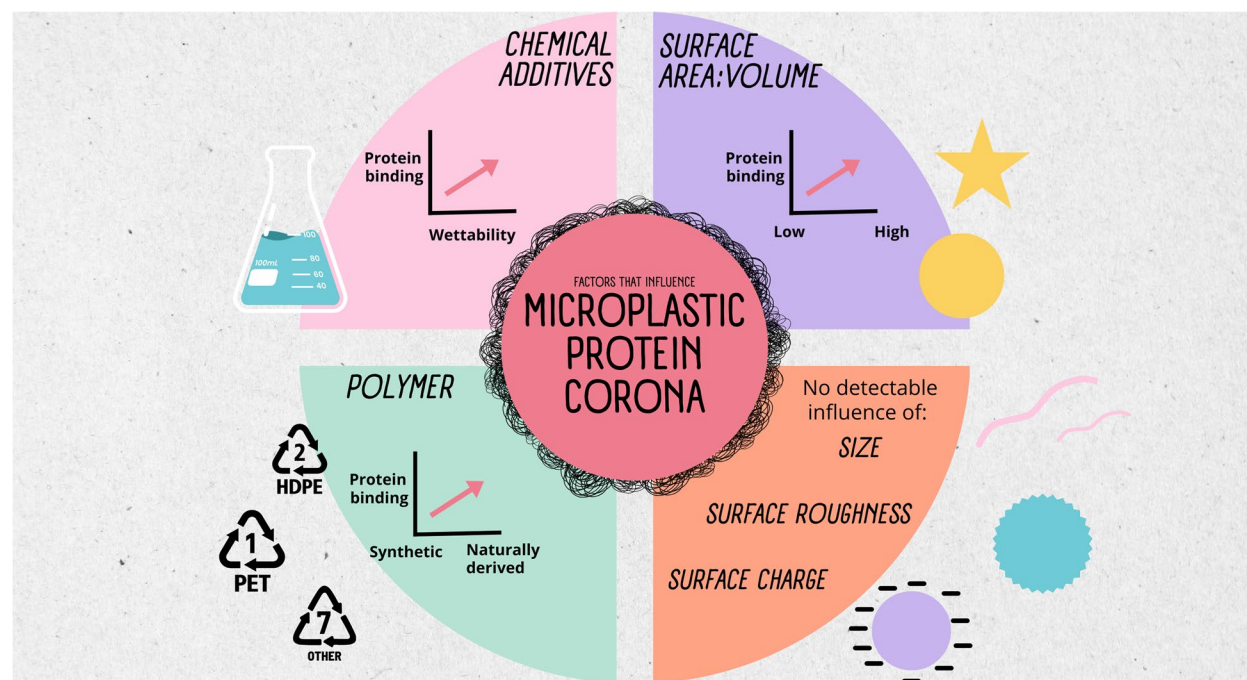
Amanda Louise Dawson
amanda.dawson@csiro.au

Full list of author information is available at the end of the article



© Crown 2024. **Open Access** This article is licensed under a Creative Commons Attribution 4.0 International License, which permits use, sharing, adaptation, distribution and reproduction in any medium or format, as long as you give appropriate credit to the original author(s) and the source, provide a link to the Creative Commons licence, and indicate if changes were made. The images or other third party material in this article are included in the article's Creative Commons licence, unless indicated otherwise in a credit line to the material. If material is not included in the article's Creative Commons licence and your intended use is not permitted by statutory regulation or exceeds the permitted use, you will need to obtain permission directly from the copyright holder. To view a copy of this licence, visit <http://creativecommons.org/licenses/by/4.0/>.

Graphical Abstract



Introduction

The expansion of macro and microplastic into the environment over the past century is well documented [1, 2]. Microplastics, in particular are isolated from every environmental compartment, including air [3], snow [4], marine and freshwater [5–7], terrestrial systems [8, 9] and the urban environment [9, 10]. Once microplastics enter the environment they undergo complex biotic and abiotic interactions. These include degradative processes such as hydrolysis, UV degradation, and mechanical abrasion [11]; chemical interactions such as sorption of environmental chemicals and contaminants, desorption of additives and/or monomers [12–14]; and biological processes such as colonisation or surface adhesion of microbiota, viruses, and extracellular polymeric substances [15–17]. Thus, understanding and quantifying these interactions can be difficult due to the multitude of dynamic environments microplastics are present in [18] and, most importantly, due to the inherent heterogeneity of microplastics themselves [11]. The all-encompassing term ‘Microplastics’ refers to a diverse suite of synthetic, semi-synthetic, and bio-polymer-based particles, often impregnated with an unknown complex mixture of chemicals.

The adsorption of extracellular polymeric substances to microplastics is thought to occur rapidly in the environment. The binding of proteins, lipids, polysaccharides,

metabolites, as well as natural organic matter, dissolved organic matter and chemical contaminants onto the surface of microplastics can form a coating known as the ecocorona [17]. Structurally, the corona is generally composed of layers, the hard corona is a tightly bound inner layer of biomolecules surrounded by a loosely associated layer, referred to as the soft corona [15].

Compared to nanoparticles, comparatively little is known about the corona formed on microplastics within the environment. Much of the knowledge regarding microplastic corona formation has been extrapolated from nanoparticle research, (e.g. [19]), however there is a need to validate these observations with microplastic particles, employing both laboratory and in situ environmental studies since physical properties such as surface area to volume ratios and surface roughness may affect corona formation considerably.

Formation of a corona on microplastic surfaces often confers vastly different properties compared with their pristine counterparts. Coronated microplastics differ in their behaviour in aqueous systems [20]. Further coronated and biofouled microplastics are associated with increased interactions with biota in terms of bioavailability, for example, vertical distribution of buoyant microplastics [21], increased ingestion [22, 23] and increased cellular interactions [24, 25]. Logically, it follows that

coronated microplastics cause altered toxicological responses in biota compared to pristine microplastics. For instance, a decreased toxicological response was observed in a recent study where *Daphnia* were exposed to polystyrene fragments derived from consumer products which were previously incubated in wastewater [26]. Conversely, Nasser and Lynch [27] demonstrated an increased toxic response in *Daphnia* exposed to polystyrene nanoparticles coated with a biomolecular corona. The toxicity mechanisms mediated by corona are not well understood, but they are extremely important for risk assessments. To better understand those mechanisms, it is essential to characterise the physicochemical properties and mechanisms that drive corona formation.

Compared to the complex and diverse ecocorona, a protein corona is formed on microplastics exposed to biological fluids. This study aimed to develop a method to extract and quantify protein comprising the hard corona formed on microplastics and explore the relationship between physical and chemical characteristics of microplastics as drivers of protein corona formation. Virgin microplastics, environmentally relevant secondary microfibres and leached secondary microfibres were incubated in a protein solution to form a corona, thereafter the hard corona was extracted and quantified using liquid chromatography combined with multiple reaction monitoring (MRM) mass spectrometry. A simple protein corona was utilised in this study for two reasons. Firstly, for to reduce complexity whilst developing extraction methods and quantification using MRM mass spectrometry, and secondly to eliminate interactions between protein and other biomolecules during corona formation.

Methods

Microplastics

This study used two groups of microplastics: virgin microplastic standards and environmentally relevant secondary microfibres. Standard microplastics used in this study were large (500–600 μm diameter) and small (53–63 μm) fluorescent red polyethylene (PE) microspheres (0.985–1.005 g cm^{-3}) (Cospheric); non-coloured polyethylene terephthalate (PET) irregular particles < 300 μm (Goodfellow); precision cut polyamide (PA) fibres (L:100 μm W:3.3 decitex (16–20 μm), 1.30–1.40 g cm^{-3}) (Goonvean); and black PET flock fibres (L:500 μm W:3.3 decitex ($\sim 17 \mu\text{m}$) (The flocking shop) (Fig. 1). Secondary microfibres were generated from clothing items using a cryogenic mill (SPEX 6775 Freezer/Mill[®]). New unwashed shirts comprising 100% recycled PET (blue), 100% PET (blue), 100% PA (black) or 100% cotton (black) were cut into 1–2 cm pieces and milled generate microfibres (see [Supplementary methods](#) for details). The clothing used in this study are widely available consumer

products, thus the milled fibres used in this study were considered environmentally relevant in terms of polymer composition (polyester, cotton and nylon), shape (fibres), and chemical content. Seams and hem stitching were avoided to ensure polymer consistency. Polymer composition of all microplastics were verified using Fourier Transform Infrared Spectroscopy (ATR-FTIR) (64 scans at 4 cm^{-1} resolution, wavenumber range = 4000–600 cm^{-1}), following methods outlined in Dawson et al. [28].

Microplastic morphology

Size, shape and particle size distribution of the virgin (PE spheres, PET fragments, PET fibres, PA fibres) and environmental (recycled PET, PET, PA and Cotton fibres) microplastics were quantified by Microtrac Sync Laser Diffraction and Dynamic Image Analysis. PE spheres, PET fragments and PET fibres were analysed as a dry powder using the TurboSync module. PA fibres and the environmental microfibres were first suspended in 100% ethanol to separate individual fibres and analysed using FlowSync with in situ sonication. Surface morphology of the microplastic standards before and after corona formation was visualised using Scanning Electron Microscopy (SEM) (TM4000 or Joel7100). Samples were either transferred directly from filter paper onto carbon tabs attached to an SEM stub or were dispersed onto a carbon tab attached to an SEM stub using a powder dispersion unit (Microtrac MJet, Germany) at 70 kPa, for 10 s. Samples were platinum sputter coated (5 nm) prior to imaging using SEM. Images were collected at either 15 kV or 2 kV using a mix of secondary and backscattered signals. Surface roughness was quantified using Atomic Force Microscopy (AFM) (Bruker ICON XR) using ScanAsyst in Air mode and SCANASYST-AIR probe (Tip radius 2 nm). Data was extracted using Nanoscope Analysis 2.0. Small PE spheres, PA fibres, PET fibres and PET fragments were suspended in 100% ethanol, dropped onto a pre-cleaned silicon wafer, and dried under vacuum. Large PE spheres were suspended in ethanol filtered onto 0.45 μm mixed cellulose ester filters (Whatman). These were then directly mounted on double sided tape and stored under vacuum until needed. Five particles for each treatment were analysed, and scan size ranged from 15 μm to 2 μm , depending on the particle size and shape. Coronated PA fibres were suspended in UltraPure distilled water and mounted as outlined above. ζ -potential of the pristine microplastics was quantified in MilliQ water using a Malvern Zetasizer Ultra. Each sample was repeated 3 times, where data was checked for quality factor and repeatability, and a mean value was taken across the 3 replicates.

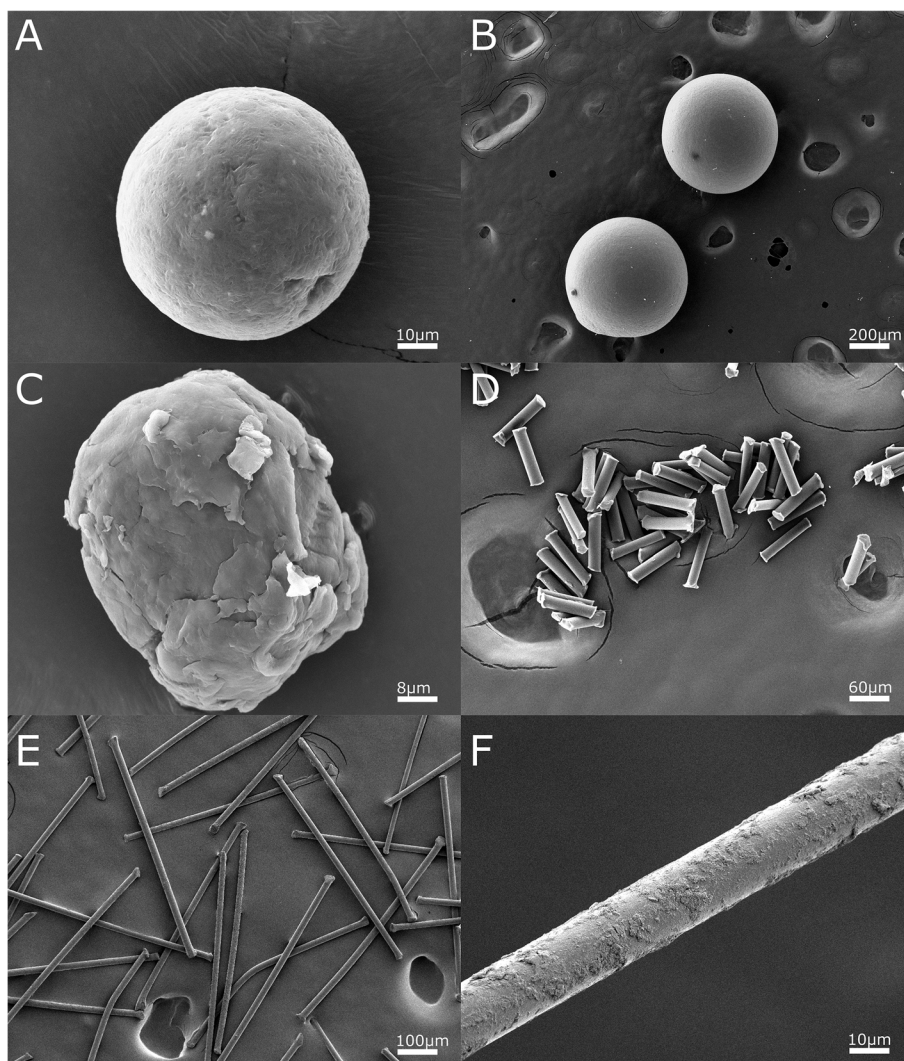


Fig. 1 Scanning electron microscopy (SEM) of standard microplastics used in this study. **A** small Polyethylene (PE) beads (x1.00k, 15 kV), **B** large PE beads (x50, 15 kV), **C** irregular Polyethylene terephthalate (PET) particles (x1.20k, 15 kV), **D** Polyamide fibres (PA) (x150, 15 kV), **E** PET flocking fibres (x100, 2.0 kV), and **F** electrostatic surface coating on PET flocking fibres (x1000, 2.0 kV)

Protein corona

Pristine microplastic fibres, fragments and spheres were incubated in sterile filtered ($0.45\ \mu\text{m}$ mixed cellulose ester Whatman) $2\ \text{mg mL}^{-1}$ aqueous Bovine Serum Albumin (BSA) solution pH 7.0 (1:4 *w:v*) for 24 h at room temperature (RT; approx. 24 degrees) on a tube roller mixer (60RPM) in the dark. Negatively buoyant microplastic suspensions (PET, PA) were then centrifuged at 10 000RCF for 15 min in an ultracentrifuge (Beckman Coulter Avanti J-26XPI) to sediment the coronated microplastics. Overlying supernatant was decanted off, and 1 mL of UltraPure distilled water was added to resuspend the pellet. The resuspended pellet was transferred to 1.5 mL LoBind protein Eppendorf tubes. These were centrifuged

at 20 800 xg, and the pellet was washed with UltraPure distilled water three times. The optimal number of washes to remove excess protein solution was determined in a pilot study (see [Supplementary Material](#)). Buoyant microplastics (PE) were extracted from the BSA solution using $40\ \mu\text{m}$ cell strainers (Corning). Microplastics captured on the strainer were flushed with pure H_2O in triplicate, and then transferred to LoBind tubes for drying, weighing and extraction.

Influence of microplastic chemical additives on corona formation

Pristine environmentally relevant synthetic microplastics, comprising of either 100% PET, 100% recycled PET

(rPET), or 100% PA, and naturally derived but anthropogenically modified microfibrils, comprised of 100% cotton, were used to analyse corona formation on realistic microplastics generated from consumer products. Consumer based plastic products contain a multitude of chemical additives which readily leach into the surrounding environment. Thus, cryomilled fibres were either used pristine or subjected to aqueous leaching to remove leachable additives. Pristine and leached fibres were incubated in 2 mg mL⁻¹ BSA solution, as outlined above, to assess the impact additives may have on the protein corona.

Microplastics (0.2 g) were leached in 2 mL of filtered MilliQ H₂O in 20 mL precleaned glass scintillation vials. Incubation consisted of 14 days at RT on an orbital shaker at 125 RPM in the dark. Glassware was precleaned by rinsing with reverse osmosis H₂O (3x), furnacing >6 h at 450 °C, then rinsing with acetone (3x) followed by dichloromethane (3x). Scintillation vial caps were rinsed with methanol (3x). MilliQ H₂O was filtered through furnaced GFC (Whatman). Glass syringes were cleaned with acetone (3x) and DCM (3x) before and after each sample. After 14d, samples were centrifuged for 10 min at 3273 RCF (Beckman Coulter Allegra X-12R). The supernatant was removed, and thereafter leached microplastics were freeze dried to remove any remaining water and stored at -20 °C until needed. Leachate composition was not quantified in this study.

Corona extraction

Washed pellets were vacuum dried, weighed, and resuspended in extraction buffer (8 M Urea, 2 M Thiourea, 4% CHAPS in 100 mM Tris-HCl, pH 8.5), sonicated for 10 min and then incubated at 900 RPM for 30 min at 22 °C. Samples were centrifuged at 20,800 xg or 15 min, and the supernatant was used for protein content analysis.

Corona extracts (70 µL) were transferred to 10 kDa molecular weight cut-off filters (Merck Millipore). The protein on the filter was washed twice with urea buffer consisting of 8 M urea in 100 M Tris-HCl (pH 8.5) with centrifugation for 15 min at 20,800 xg. Then, it was incubated with 50 mM DTT in urea buffer for 30 min at RT shaking at 300 RPM. Filters were then rewashed with urea buffer twice before adding Iodoacetamide (50 mM, 100 µL) in urea buffer and incubated in the dark for 30 min before centrifugation at 19,745 RCF for 15 min. The buffer was exchanged with 100 mM ammonium bicarbonate (pH 8.0) with two consecutive wash/centrifugation cycles. The filters were transferred to fresh collection tubes. The extracted protein was digested overnight at 37 °C with 200 µL of sequence grade (Promega) bovine trypsin (250 µg mL⁻¹ in 100 mM ammonium

bicarbonate (pH 8.0)). Thereafter, filters were centrifuged for 15 min at 20,800 xg, washed twice with 200 µL of 100 mM ammonium bicarbonate, then dried by vacuum concentration and resuspended in 25 µL of 0.1% formic acid.

Negative controls were prepared for all experiments in triplicate for each polymer. These comprised of unexposed microplastic particles extracted and quantified alongside samples.

Liquid chromatography and mass spectrometry analysis

Digested peptides (1 µL) were separated with a Shimadzu Nexera UHPLC system equipped with a Kinetex C18 column following Nelis et al. [29]. BSA peptide data and multiple reaction monitoring method development are outlined in Colgrave et al. [30]. Multiple reaction monitoring transitions for the five most abundant BSA peptides used in this study are summarised in Table S1.

Protein concentration

Microplastic leachates present in the flocking fibre and shirt fibre protein extracts interfered with spectroscopic protein quantification (i.e., Bradford assay). Thus, calibration curves using known standards were developed to determine the concentration of protein bound to the coronated microplastics. Pure BSA protein (8.078 mg mL⁻¹) was extracted using the above method and a calibration curve was prepared at concentrations spanning 0.5–1000 µg mL⁻¹. The mass of protein forming a hard corona on the unknown extracted samples and negative controls was determined by interpolating the peak areas of the most abundant transition of the most abundant peptide identified in the MRM method on the calibration curve. An ion ratio (IR) was combined with the retention time to identify peptides unambiguously. The ion ratio was accepted under the following conditions: variance was 20% if IR > 0.5, 25% if 0.2 < IR < 0.5, and 30% if 0.1 < IR < 0.2. For the LOQ and LOD, a signal-to-noise ratio > 3 and 10 was used, respectively. The quantifying peak was integrated for quantification if the IR, retention time and signal-to-noise ratio criteria were fulfilled. Protein concentration was normalised by the extracted microplastic dry weight (µg mg⁻¹ plastic).

Data analysis

Skyline v21.1.0.146 was used for mass spectral analysis. GraphPad 9.2.0 was used for statistical analyses. ANOVA with Tukey's multiple comparison tests determined significant differences between protein concentrations. T-tests were used to compare protein concentration and zeta potential differences between pristine and leached microfibrils. Normality was assessed using Shapiro-Wilk tests. Simple linear regression was used to explore the

relationship between microplastics characteristics and protein corona concentration.

Results and discussion

Protein corona

Microplastic standards

BSA protein was detected in all microplastic samples after incubation, suggesting that a hard corona had formed on the particles over the 24 h period (Figure S2). Overall, there was no significant difference between the protein concentration quantified using the five BSA peptides (AEFVEVTK, LVTDLTK, LVNELTEFAK, SLHTLF-GDELCK, and YLYEIAR) for all plastics, except for the small PE beads ($p < 0.05$, $F_{(4, 10)} = 4.893$) (Figure S3). Protein quantification using peptide LVNELTEFAK resulted in minimal variation across replicates in the small bead samples, and performed consistently across all 5 plastic types. Thus, LVNELTEFAK was selected for all further comparative analysis in this study. Additionally, the result for each individual peptide is presented in Figure S4 for comparison.

The protein concentration extracted from the corona of each sample was significantly different (Table S2, Fig. 2A, $p < 0.0001$, $F_{(4, 10)} = 56.96$), with PET fibres having the highest concentration of protein overall ($3.59 \pm 0.27 \mu\text{g mg}^{-1}$ plastic). Interestingly, there were significant differences between both the small ($1.4 \pm 0.10 \mu\text{g mg}^{-1}$ plastic) and large PE beads ($0.19 \pm 0.04 \mu\text{g mg}^{-1}$ plastic) ($p < 0.05$), and between the PET fibres ($3.59 \pm 0.27 \mu\text{g mg}^{-1}$ plastic) and fragments ($2.4 \pm 0.52 \mu\text{g mg}^{-1}$ plastic) ($p < 0.001$), suggesting that protein adsorption, and thus, corona formation may not have been influenced by polymer type. However further study may be needed elucidate the influence of polymer. Both the PET fibres and large PE beads had a similar maximum length of $500 \mu\text{m}$ (Table S2),

whereas PET fibres had the highest protein concentration extracted, large beads had the lowest, suggesting that, just as with nanoparticles [31], shape, rather than length, may be an important driver of corona formation.

Protein aggregates were visible on the surface of the small PE beads and PET fibres under brightfield microscopy (100x magnification, Figure S5). However, when microplastics were filtered onto paper for SEM imaging, no visible protein aggregates were visible (Figures S5 and S6). Thus, it is likely that the aggregates were not well attached to the surface and were dislodged during filtration. It is possible that these aggregates formed the soft corona, instead of the tightly bound hard corona. The surface morphology of pristine PE and PET microplastics were heterogenous. PET microplastics (PET fibres: $36.10 \pm 14.03 \text{ nm}$, PET fragments: $42.88 \pm 29.61 \text{ nm}$) were slightly smoother than PE beads (small PE: $96.46 \pm 17.75 \text{ nm}$, large PE: $62.98 \pm 13.03 \text{ nm}$) (Fig. 3; Figure S7). Conversely, the surface of pristine PA fibres ($5.24 \pm 1.45 \text{ nm}$) exhibited symmetrical ridges running the length of the fibres (Fig. 4) and was significantly less rough than both PE beads and the PET fragments ($F_{(4, 21)} = 18.74$, $p < 0.0001$). The irregular surface texture on the PE and PET microplastics was likely to obscure the detection of adsorbed BSA protein. Therefore, only PA fibres were selected to further examine surface attachment of the BSA protein using atomic force microscopy. The cross-section height of the pristine fibres was reasonably symmetrical (Fig. 4A, C,E). However, after corona formation on the fibres, the characteristic ridges became obscured and were barely detectable (Fig. 4B, D,F). The cross-section height of the PA surface after adsorption revealed the BSA did not bind uniformly across the surface, producing a heterogenous surface with protein aggregations. Although these were notably smaller than

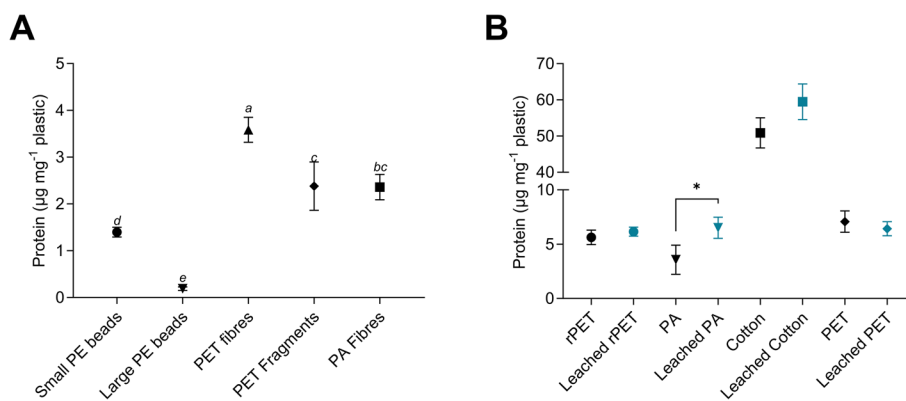


Fig. 2 Concentration of BSA protein forming a corona on each polymer measured by LC-MRM-MS. **A** Virgin microplastic standards and **(B)** Leached (blue) and pristine (black) environmental microfibrils. Letters (ANOVA, $p < 0.05$) and asterisks (t-test, $p < 0.05$) denote statistically significant differences

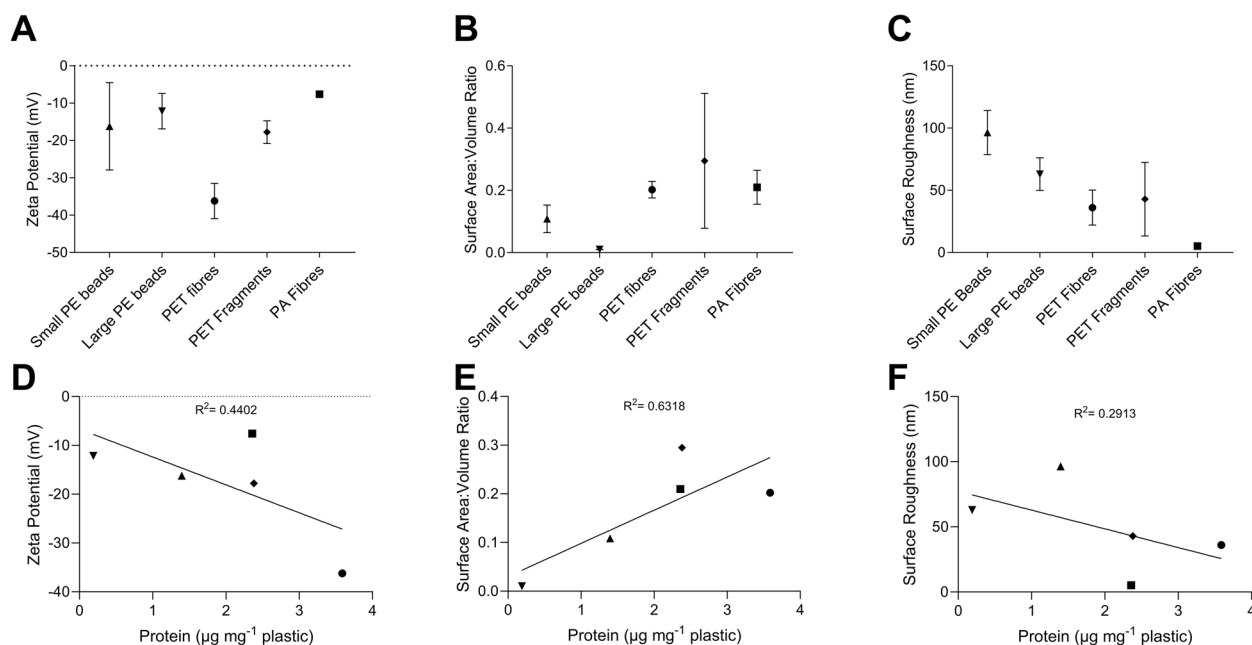


Fig. 3 **A** Zeta potential and **(B)** Surface Area to Volume ratio; and **(C)** Surface roughness for all five microplastic types with corona protein concentration **(D-F)**

the aggregations visible on the small PE beads and PET fibres in Figure S5.

All microplastics, except PET fibres, were unstable in solution, with zeta potentials less than -30 mV (Table S2). The small PE beads, in particular, exhibited large variation between replicates, with values trending towards zero over successive replicates (Fig. 3A, Figure S8), suggesting the low density PE beads were generally unstable in water, floating toward the surface and possibly aggregating. For all microplastics, length ($F_{(1,3)}=0.2134$, $R^2=0.0664$), width ($F_{(1,3)}=6.055$, $R^2=0.6687$), surface area: volume ratio (SA: Vol) ($F_{(1,3)}=5.148$, $R^2=0.6318$), surface roughness ($F_{(1,3)}=1.233$, $R^2=0.2913$) and zeta potential ($F_{(1,3)}=2.359$, $R^2=0.4402$) did not significantly influence corona protein concentration ($p>0.05$). However, PET fibres were noted to have significantly higher zeta potential than all other microplastics ($p<0.01$, $F_{(4,10)}=9.341$) and were also associated with the highest protein concentration.

Flocking fibres are treated to enhance surface conductivity, thus allowing them to accept an electric charge and facilitate electrostatic application to surfaces [32]. The PET flock fibres used in this study were surface treated with an unknown additive (Fig. 1F; Figure S7D). Electrostatic surface coatings typically increase conductivity and hydrophilicity, which may explain the significantly higher zeta potential and possibly the increased protein corona formation. When the PET flock fibres were excluded from analysis, SA: Vol was found to have a significant

positive relationship with corona protein concentration ($p<0.05$, $F_{(1,2)}=19.02$, $R^2=0.9048$), suggesting SA: Vol is a contributing factor for protein corona formation on microplastics which are not treated with electrostatic additives.

This corresponds well with observations of nanoparticle protein adsorption [31, 33], where increased surface area to volume ratio facilitates increased protein binding. Microplastics, too, follow this relationship. A recent study quantified the protein corona on microplastic beads under synthetic digestion conditions [34]. The study reported an elevated protein concentration compared to the present study (25.32 ± 8.84 $\mu\text{g mg}^{-1}$ of protein). Yet, the beads used were approximately 10 times smaller than the beads used in this study (5 μm polystyrene (PS) beads and 50 μm PE beads, respectively), thus following the relationship of protein binding in function of SA: Vol displayed in the present study.

In the case of nanoparticles, surface roughness also influences protein adsorption. In particular, particles with a smooth surface have been associated with higher BSA adsorption [31]. However, in the current study, surface roughness did not appear to strongly influence the concentration of protein adsorbed to the polymer surface. Figure 3 shows a slight relationship between surface roughness and protein concentration. For example, PA fibres were significantly smoother than both the PE beads and the PET fragments $p<0.05$; $F_{(4,21)}=18.74$) and were associated with a high protein corona concentration

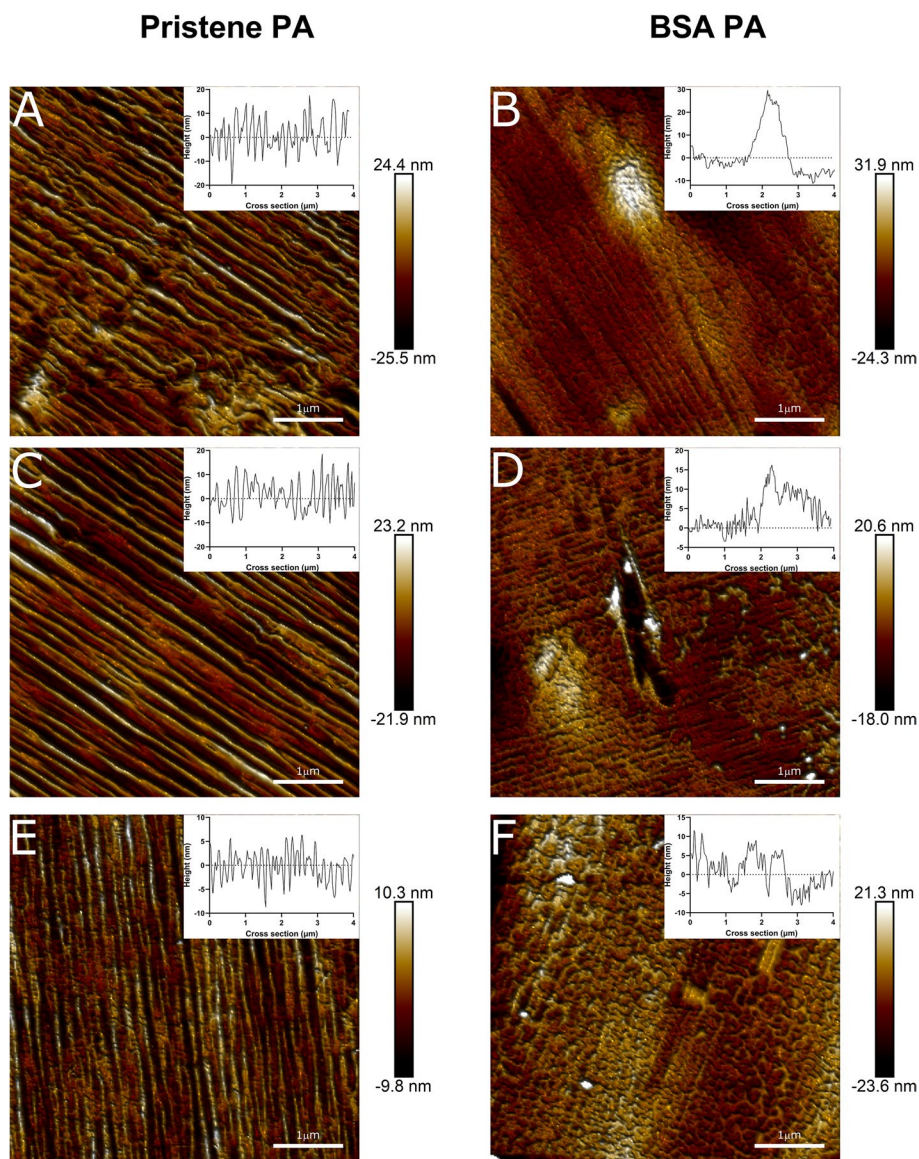


Fig. 4 Surface morphology of pristine (**A**, **C** and **E**) and BSA coronated (**B**, **D** and **F**) polyamide (PA) fibres. Inserts show the cross-section height of the surface, measured perpendicular to the elongated ridges. Atomic force microscopy scan areas were 5 μm . Colour bars indicate surface height

(Fig. 2), but overall surface roughness appeared to be a minor driver compared with additive content and SA: Vol (Fig. 3).

Environmentally relevant microfibrils

The fibre width was consistent across the four clothing types, ranging from cotton (14.67 ± 9.39) to PA (19.70 ± 15.25 μm). After milling, the mean fibre length for all four polymers were approximately 40–50 μm (Table S2). However, due to the cyromilling process the length varied considerably (rPET: 4.23–704.1 μm , PET: 4.05–1394 μm , PA: 4.18–932.5 μm , and Cotton:

4.25–414.6 μm) (Figure S9). Thus, the surface area to volume ratio of each polymer was also quite variable (Fig. 5A). After 14 days of aqueous leaching, the aqueous media surrounding the cotton and PA microfibrils were noted to have changed colour from clear to black and brown, respectively, indicating that the black dye present within each fabric, and possibly other chemical additives, had leached from the fibres into the media. Therefore, providing a visual confirmation of chemical leaching from the microfibrils under ambient conditions. The four environmentally relevant fibres were more stable in solution than the microplastic standards,

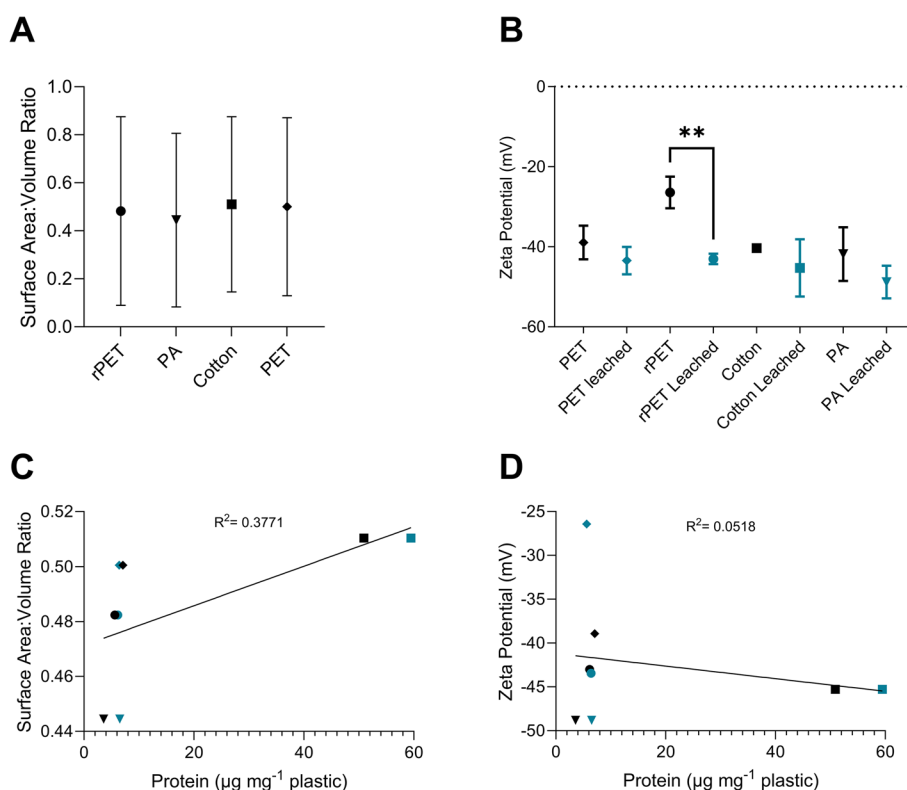


Fig. 5 **A** Surface Area to Volume ratio and **(B)** Zeta potential of the pristine (black) and leached (blue) microfibres, and their relationship with corona protein concentration **(C, D)**, (t-test $**p < 0.01$, $t_{(4)} = 6.924$)

with zeta potentials of approximately -40 mV for most fibres. The only exception was rPET, which had a significantly lower zeta potential than PET, PA and Cotton fibres ($p < 0.01$, $F_{(3, 8)} = 7.644$). However, leaching significantly increased the stability of these fibres ($p < 0.01$, $t_{(4)} = 6.924$). Zeta potential of the rPET increased from -26.42 to -43.01 mV after aqueous leaching. Indeed, all fibres had a slightly increased zeta potential after leaching (Fig. 5, Figure S10).

BSA protein corona was extracted and quantified from all the textile microfibre samples (Table S2). Cotton microfibres had a significantly higher protein concentration than the three synthetic microplastics ($p < 0.0001$, $F_{(3,8)} = 301.6$). The protein extracted from the cotton microfibres ($50.9 \pm 4.16 \mu\text{g mg}^{-1}$ plastic) was around 10 times higher than the protein extracted from rPET ($5.63 \pm 0.67 \mu\text{g mg}^{-1}$ plastic), PET ($7.08 \pm 0.99 \mu\text{g mg}^{-1}$ plastic), and PA ($3.57 \pm 1.34 \mu\text{g mg}^{-1}$ plastic). To confirm that the elevated protein content of the cotton fibres was not due to the presence of the quantification peptide, LVNELTEFAK, in cotton or in organisms which may be present on cotton, BLASTp[®] was used to search for identical peptide matches using the non-redundant protein sequence database (UniProt) without species restrictions.

No reasonable matches were identified. Thus, two hypotheses for the elevated protein concentration in the cotton samples are suggested below. Firstly, the protein extraction efficiency for cotton may be more comprehensive. It was noted that after incubation in the extraction buffer, cotton had completely lost all fibrous structure. The resulting material had the appearance of a thick sludge, suggesting a complete breakdown of the fibres, which may have aided the release of BSA from the particles. Secondly, Cotton fibres are hydrophilic and absorb water [35]. The wettability of these fibres may have facilitated protein adsorption compared to the hydrophobic synthetic fibres.

Conversely, pristine PA exhibited the lowest concentration of protein. However, leaching significantly increased protein corona formation on the PA microplastics. The corona formed on leached PA fibres was almost double that of the pristine, with $3.57 \pm 1.34 \mu\text{g BSA per mg plastic}$ and $6.51 \pm 0.97 \mu\text{g BSA per mg plastic}$, extracted from the pristine and leached microfibres respectively (Fig. 2B, $p < 0.05$, $t_{(4)} = 3.086$). Cotton also followed this trend of increasing protein corona formation on leached microfibres ($50.90 \pm 4.18 \mu\text{g mg}^{-1}$ plastic and $59.49 \pm 4.92 \mu\text{g mg}^{-1}$ plastic for pristine and leached

fibres respectively), but the increase was non-significant ($p=0.08$, $t_{(4)}=2.304$).

The PA fibres were generated from a shirt which was advertised as a water-repellent outer activewear. The chemical additive/s used to give the garment water-repelling properties likely reduced the wettability of the fibres, thus hindering the formation of a protein corona in the aqueous media. However, this effect was diminished in the leached fibres, which suggests the additive was leached from the garment under aqueous conditions. Interestingly, leaching also led to an increased zeta potential for all fibres, and thus, stability within the BSA suspension was also likely increased. Yet, this increased stability did not seem to translate to increased protein corona formation, as the largest zeta potential increase was observed in the rPET (Fig. 5B) but the largest increase in protein concentration of leached microplastics was observed on PA fibres (Fig. 2B).

There was no significant relationship between the microfibre protein concentration and SA: Vol or zeta potential ($p>0.05$, $F_{(1,6)}=3.632$, $R^2=0.3771$; and $F_{(1,6)}=0.3278$, $R^2=0.0518$, respectively), even if cotton was excluded from the analysis as an outlier ($F_{(1,4)}=2.329$, $R^2=0.3680$). Thus, for microplastics derived from consumer products, additives are proposed to be the dominant force influencing protein BSA corona formation.

In this study, leaching was carried out over 14 days but recent studies have shown the rapid leaching of additives from microplastics upon entering aqueous environments [36], any derived effects of reduced wettability due to additive content will presumably be short-lived once microplastics enter aqueous environments. Theoretically, leaving them unhindered to adsorb exoproteins and form an ecocorona.

Textile fibres are prolifically shed from garments [37–39]. Machine laundering of textiles have been seen to release 128–1054 mg kg⁻¹ of fibres to wastewater [37]. Although wastewater treatment facilities are highly effective at removing microplastics [40], numerous microfibrils are released into the environment in treated wastewater [41]. The protein rich biological fluids present in wastewater present considerable opportunities for ecocorona formation as microplastics transit through wastewater systems, before being released, either as biosolids or treated wastewater. It is currently unknown how the presence of an ecocorona may alter the transport, fate, and toxicity of microplastics after their release into the environment from wastewater treatment facilities. Although valuable contributions have been made in this field. Schur et al. [26] evaluated the multigenerational toxicity of wastewater incubated PS microplastics to *Daphnia magna*. The study found wastewater incubated particles were less lethal over successive generations and

proposed that pristine microplastics may be more toxic than ecocoronated microplastics.

The fibres used in this study were exposed to a single protein solution only, forming a simplified protein corona, rather than a complex ecocorona. In more complex environmental scenarios, the layer of molecules forming the soft corona is capable of dynamically exchanging molecules depending on the environment [17, 42]. Therefore, if ecocoronated microplastics are ingested, the labile soft corona is likely to reflect the current conditions in the environment. Organisms are, therefore, likely to be pre-exposed, and in terms of organic contaminants, possibly at equilibrium [43], with the components of this layer. However, once formed, the hard corona is considerably less dynamic, and have the capacity to retain molecules from different environmental compartments [15]. Thus, the hard corona may be of particular relevance as a potential exposure pathway for foreign biomolecules and contaminants. Consequently, it would be pertinent to expose textile microfibrils to dynamic environmental solutions to elucidate ecocorona characteristics and potential toxicity.

Textile fibres also comprise a significant component of household dust [44]. Regular everyday use, (e.g. [37]), as well as tumble drying, (e.g. [45]), cause fibres to be shed into indoor environments, where they can be inhaled [46], settle onto foodstuff and indirectly ingested [47], or be indirectly ingested through hand to mouth activity [48]. Due to this abundance, textile microfibrils may be one of the highest exposure sources of microplastic to humans. Thus, the toxicological effects of human exposure to microfibrils may be highly pertinent. Notably, a recent study examined *in situ* protein corona formation on microplastics during *in vitro* human digestion [34]. Microplastics subjected to the model formed a corona comprising digestive fluid proteins. Interestingly, when these microplastics were used in toxicity assays, coronated microplastics had a reduced toxic effect on human intestinal cells compared to pristine PS beads. In the current study, textile microfibrils adsorbed significantly higher concentrations of protein than fragments and spheres of similar size and demonstrated a strong dependence upon chemical additives, both traits are likely to alter the toxicity of microfibrils compared to laboratory beads.

Conclusions

Overall, corona formation on microplastics remains understudied, and coronated microplastics remain underutilised in toxicity studies. It is known from the substantial body of research on nanomaterials that the presence of an eco- or protein corona confers a new biological identity to particles, which may be likely

to interact with cells, differ in aqueous stability and increase aggregation. All microplastics in this study, including hydrophobic textile microfibrils, formed a protein corona after 24 h incubation. When microplastics are relatively free of chemical additives surface area to volume ratio plays an important role in influencing the protein binding. Yet, when chemical additives were present within the polymer, surface area to volume ratio was no longer the significant physicochemical attribute influencing protein corona formation. Regardless of additive content, the naturally derived cotton sorbed a significantly higher concentration of protein than the synthetically derived polymers. As most microplastics in the environment are derived from consumer products, chemical additives are likely to play a critical role in corona formation in the environment. Building off these findings, future studies could utilise untargeted mass spectrometry workflows to identify which chemical additives within clothing fibres which may be responsible for the observations reported in this study.

Abbreviations

PE	Polyethylene
PET	Polyethylene terephthalate
rPET	Recycled polyethylene terephthalate
PA	Polyamide
FTIR	Fourier Transform Infrared Spectroscopy
SEM	Scanning Electron Microscopy
RT	Room temperature
BSA	Bovine Serum Albumin
RCF	Relative centrifugal force
MRM	Multiple reaction monitoring
LOQ	Limits of quantification
LOD	Limits of detection
IR	Ion ratio
SA	Vol surface area to volume ratio
PS	Polystyrene

Supplementary Information

The online version contains supplementary material available at <https://doi.org/10.1186/s43591-024-00086-6>.

Supplementary Material 1.

Acknowledgements

This work used the Queensland node of the NCRIS-enabled Australian National Fabrication Facility (ANFF). The authors would like to acknowledge the Turrbal and Jagera peoples as the Traditional Owners of the country on which this work was carried out at CSIRO, St. Lucia.

Supporting information

Supporting information for this study: Pilot study outline and results; peptide transition list, interpolated recovery, and total concentration for each polymer type; micrographs of attached protein; and correlations between polymer physicochemical characteristics and protein.

Authors' contributions

AD conceptualised the study, designed the study and acquired data; AD, JN and UB interpreted the data; AD, JN, UB and DN contributed to the drafting and revising the study.

Funding

AD and JN were supported by a Research Plus CERC postdoctoral fellowship by CSIRO, Australia. DN was supported by Winanga-y postdoctoral fellowship from CSIRO.

Availability of data and materials

Data from this publication is available at <https://doi.org/10.5281/zenodo.10202428>.

Declarations

Ethics approval and consent to participate

No ethical requirements were needed for this study.

Consent for publication

All authors are aware of the manuscript and give consent to publish.

Competing interests

The authors declare no competing interests.

Author details

¹CSIRO Agriculture and Food, 306 Carmody Rd, St Lucia, QLD 4067, Australia.

²Australian Research Council Centre of Excellence for Innovations in Peptide and Protein Science, School of Science, Edith Cowan University, 270 Joondalup Dr, Joondalup, WA 6027, Australia.

Received: 30 November 2023 Accepted: 21 March 2024

Published online: 17 April 2024

References

- Liu L-Y, Mai L, Zeng EY. Plastic and Microplastic Pollution: from Ocean Smog to Planetary Boundary threats. In: Jiang G, Li X, editors. A New Paradigm for Environmental Chemistry and Toxicology: from concepts to insights. Singapore: Springer Singapore; 2020. pp. 229–40.
- Galloway TS, Lewis CN. Marine microplastics spell big problems for future generations. *Proc Natl Acad Sci.* 2016;113(9):2331–3.
- Sridharan S, Kumar M, Singh L, Bolan NS, Saha M. Microplastics as an emerging source of particulate air pollution: a critical review. *J Hazard Mater.* 2021;418:126245.
- Zhang Y, Gao T, Kang S, Shi H, Mai L, Allen D, et al. Current status and future perspectives of microplastic pollution in typical cryospheric regions. *Earth Sci Rev.* 2022;226:103924.
- Triebkorn R, Braunbeck T, Grummt T, Hanslik L, Huppertsberg S, Jekel M, et al. Relevance of nano- and microplastics for freshwater ecosystems: a critical review. *TrAC Trends Anal Chem.* 2019;110:375–92.
- Talbot R, Chang H. Microplastics in freshwater: a global review of factors affecting spatial and temporal variations. *Environ Pollut.* 2022;292:118393.
- Lindeque PK, Cole M, Coppock RL, Lewis CN, Miller RZ, Watts AJR, et al. Are we underestimating microplastic abundance in the marine environment? A comparison of microplastic capture with nets of different mesh-size. *Environ Pollut.* 2020;265:114721.
- Baho DL, Bundschuh M, Futter MN. Microplastics in terrestrial ecosystems: moving beyond the state of the art to minimize the risk of ecological surprise. *Glob Change Biol.* 2021;27(17):3969–86.
- Campanale C, Galafassi S, Savino I, Massarelli C, Ancona V, Volta P, et al. Microplastics pollution in the terrestrial environments: poorly known diffuse sources and implications for plants. *Sci Total Environ.* 2022;805:150431.
- Qiu R, Song Y, Zhang X, Xie B, He D. Microplastics in Urban environments: sources, pathways, and distribution. In: He D, Luo Y, editors. *Microplastics in Terrestrial environments: emerging contaminants and Major challenges.* Cham: Springer International Publishing; 2020. pp. 41–61.
- Andrady AL. The plastic in microplastics: a review. *Mar Pollut Bull.* 2017;119(1):12–22.
- Zimmermann L, Bartosova Z, Braun K, Oehlmann J, Völker C, Wagner M. Plastic products Leach Chemicals that Induce in Vitro toxicity under realistic Use conditions. *Environ Sci Technol.* 2021;55(17):11814–23.

13. Wiesinger H, Wang Z, Hellweg S. Deep dive into Plastic monomers, additives, and Processing Aids. *Environ Sci Technol.* 2021;55(13):9339–51.
14. Torres FG, Dioses-Salinas DC, Pizarro-Ortega CI, De-la-Torre GE. Sorption of chemical contaminants on degradable and non-degradable microplastics: recent progress and research trends. *Sci Total Environ.* 2021;757:143875.
15. Galloway TS, Cole M, Lewis C. Interactions of microplastic debris throughout the marine ecosystem. *Nat Ecol Evol.* 2017;1(5):116.
16. Zettler ER, Mincer TJ, Amaral-Zettler LA. Life in the plastisphere: microbial communities on plastic marine debris. *Environ Sci Technol.* 2013;47(13):7137–46.
17. Wheeler KE, Chetwynd AJ, Fahy KM, Hong BS, Tochihiuti JA, Foster LA, et al. Environmental dimensions of the protein corona. *Nat Nanotechnol.* 2021;16(6):617–29.
18. Reilly K, Davoudi H, Guo Z, Lynch I. The composition of the Eco-corona acquired by Micro- and Nanoscale Plastics impacts on their ecotoxicity and interactions with co-pollutants. In: Szpunar J, Jiménez-Lamana J, editors. *Environmental nanopollutants: sources, occurrence, analysis and fate.* The Royal Society of Chemistry; 2022. p. 0.
19. Cao J, Yang Q, Jiang J, Dalu T, Kadushkin A, Singh J, et al. Coronas of micro/nano plastics: a key determinant in their risk assessments. *Part Fibre Toxicol.* 2022;19(1):55.
20. Schwartz M, Saudrais F, Devineau S, Chédin S, Jamme F, Leroy J, et al. Role of the Protein Corona in the Colloidal Behavior of Microplastics. *Langmuir.* 2023;39(12):4291–303.
21. Porter A, Lyons BP, Galloway TS, Lewis C. Role of Marine snows in Microplastic Fate and Bioavailability. *Environ Sci Technol.* 2018;52(12):7111–9.
22. Savoca MS, Tyson CW, McGill M, Slager CJ. Odours from marine plastic debris induce food search behaviours in a forage fish. *Proc Royal Soc B: Biol Sci.* 1860;2017(284):20171000.
23. Vroom RJE, Koelmans AA, Besseling E, Halsband C. Aging of microplastics promotes their ingestion by marine zooplankton. *Environ Pollut.* 2017;231:987–96.
24. Jasinski J, Wilde MV, Voelkl M, Jérôme V, Fröhlich T, Freitag R, et al. Tailor-made protein Corona formation on polystyrene microparticles and its Effect on Epithelial Cell Uptake. *ACS Appl Mater Interfaces.* 2022;14(41):42777–87.
25. Ramsperger AFRM, Narayana VKB, Gross W, Mohanraj J, Thelakkat M, Greiner A, et al. Environmental exposure enhances the internalization of microplastic particles into cells. *Sci Adv.* 2020;6(50):eabd1211.
26. Schür C, Weil C, Baum M, Wallraff J, Schreier M, Oehlmann J, et al. Incubation in Wastewater reduces the multigenerational effects of Microplastics in *Daphnia magna*. *Environ Sci Technol.* 2021;55(4):2491–9.
27. Nasser F, Lynch I. Secreted protein eco-corona mediates uptake and impacts of polystyrene nanoparticles on *Daphnia magna*. *J Proteom.* 2016;137:45–51.
28. Dawson AL, Santana MFM, Nelis JLD, Motti CA. Taking control of microplastics data: a comparison of control and blank data correction methods. *J Hazard Mater.* 2023;443:130218.
29. Nelis JLD, Dawson AL, Bose U, Anderson A, Colgrave ML, Broadbent JA. Safe food through better labelling; a robust method for the rapid determination of caprine and bovine milk allergens. *Food Chem.* 2023;417:135885.
30. Colgrave ML, Byrne K, Caine J, Kowalczyk L, Vibhakaran Pillai S, Dong B, et al. Proteomics reveals the in vitro protein digestibility of seven transmembrane enzymes from the docosahexaenoic acid biosynthesis pathway. *Food Chem Toxicol.* 2019;130:89–98.
31. Bilardo R, Traldi F, Vdovchenko A, Resmini M. Influence of surface chemistry and morphology of nanoparticles on protein corona formation. *WIREs Nanomed Nanobiotechnol.* 2022;14(4):e1788.
32. McCarthy A, Shah R, John JV, Brown D, Xie J. Understanding and utilizing textile-based electrostatic flocking for biomedical applications. *Appl Phys Reviews.* 2021;8(4):041326.
33. Kamaly N, Farokhzad OC, Corbo C. Nanoparticle protein corona evolution: from biological impact to biomarker discovery. *Nanoscale.* 2022;14(5):1606–20.
34. Liu S, Wu X, Gu W, Yu J, Wu B. Influence of the digestive process on intestinal toxicity of polystyrene microplastics as determined by in vitro Caco-2 models. *Chemosphere.* 2020;256:127204.
35. Moriam K, Rissanen M, Sawada D, Altgen M, Johansson L-S, Evtugin DV, et al. Hydrophobization of the Man-made cellulosic fibers by incorporating Plant-Derived Hydrophobic compounds. *ACS Sustain Chem Eng.* 2021;9(13):4915–25.
36. Gulizia AM, Patel K, Philippa B, Motti CA, van Herwerden L, Vamvounis G. Understanding plasticiser leaching from polystyrene microplastics. *Sci Total Environ.* 2023;857:159099.
37. De Falco F, Cocca M, Avella M, Thompson RC. Microfiber Release to Water, Via laundering, and to Air, via Everyday Use: a comparison between Polyester Clothing with Differing Textile Parameters. *Environ Sci Technol.* 2020;54(6):3288–96.
38. Athey SN, Adams JK, Erdle LM, Jantunen LM, Helm PA, Finkelstein SA, et al. The widespread environmental footprint of Indigo Denim microfibers from Blue jeans. *Environ Sci Technol Lett.* 2020;7(11):840–7.
39. Tiffin L, Hazlehurst A, Sumner M, Taylor M. Reliable quantification of microplastic release from the domestic laundry of textile fabrics. *J Text Inst.* 2022;113(4):558–66.
40. Frehland S, Kaegi R, Hufenus R, Mitrano DM. Long-term assessment of nanoplastic particle and microplastic fiber flux through a pilot wastewater treatment plant using metal-doped plastics. *Water Res.* 2020;182:115860.
41. Napper IE, Parker-Jurd FNF, Wright SL, Thompson RC. Examining the release of synthetic microfibres to the environment via two major pathways: Atmospheric deposition and treated wastewater effluent. *Sci Total Environ.* 2023;857:159317.
42. Hadjidemetriou M, Kostarelou K. Evolution of the nanoparticle corona. *Nat Nanotechnol.* 2017;12(4):288–90.
43. Koelmans AA, Bakir A, Burton GA, Janssen CR. Microplastic as a Vector for Chemicals in the aquatic environment: critical review and model-supported reinterpretation of empirical studies. *Environ Sci Technol.* 2016;50(7):3315–26.
44. Perera K, Ziajahromi S, Nash SB, Leusch FDL. Microplastics in Australian indoor air: abundance, characteristics, and implications for human exposure. *Sci Total Environ.* 2023;889:164292.
45. O'Brien S, Okoffo ED, O'Brien JW, Ribeiro F, Wang X, Wright SL, et al. Airborne emissions of microplastic fibres from domestic laundry dryers. *Sci Total Environ.* 2020;747:141175.
46. Vianello A, Jensen RL, Liu L, Vollertsen J. Simulating human exposure to indoor airborne microplastics using a Breathing Thermal Manikin. *Sci Rep.* 2019;9(1):8670.
47. Dawson AL, Li JYQ, Kroon FJ. Plastics for dinner: store-bought seafood, but not wild-caught from the great barrier reef, as a source of microplastics to human consumers. *Environ Adv.* 2022;8:100249.
48. Soltani NS, Taylor MP, Wilson SP. Quantification and exposure assessment of microplastics in Australian indoor house dust. *Environ Pollut.* 2021;283:117064.

Publisher's Note

Springer Nature remains neutral with regard to jurisdictional claims in published maps and institutional affiliations.